Research Article **Open Access**

Hugo Mercado-Mendoza and Sylvie Lorente*

Impact of the pore solution on the aqueous diffusion through porous materials

Abstract: This paper reviews the main advances of our group on the measurements of the diffusion coefficient through partially saturated porous materials. The technique that we developed is based on the definition of an equivalent electrical model reproducing the behavior of the porous microstructure. The electrical characteristics are measured by means of Electrochemical Impedance Spectroscopy. After validating the approach on saturated samples, the method was applied to partially saturated materials. We showed that the pore solution ionic composition has not impact on the results, and documented the effect of the pore size distribution on the macroscopic diffusion coefficient.

Keywords: porous media, pore network, saturation level, diffusion

DOI 10.1515/eng-2015-0013
Received October 31, 2014; accepted January 05, 2015

1 Introduction

The diffusion coefficient is a macroscopic parameter that depends on the characteristics of both the diffusing species and the porous material involved in the diffusion process [1–3]. This parameter is of extreme importance in several domains. In nuclear engineering, the confinement of nuclear waste is done by means of cement-based materials, and its success depends on knowing the diffusion coefficient. In civil engineering applications, species such as chloride may invade the pore network of the material, reach the reinforcement bars of concrete structures and trigger the initiation of corrosion.

Most techniques rely still today on saturated samples [1, 4–11]. Yet, in-situ structures are hardly encountered in saturated state. There is a strong need, not only in the domain of civil engineering but also in nuclear engineering and nuclear waste disposal, to determine the relationship between aqueous diffusion coefficients and the saturation level of the materials. The objective of this paper is to review the progress made by our group in developing a technique based on Electrochemical Impedance Spectroscopy to determine the diffusion coefficient through non saturated porous materials.

2 Materials and methods

Two different kinds of materials were tested: TiO_2 samples as non-reactive porous material and cement pastes samples as reactive porous systems. The TiO_2 ceramics was chosen for being inert vis-à-vis chloride and alkali ions, unlike concrete. Their geometry was cylindrical (110 mm in diameter, 15 mm in thickness). The cement paste samples were based on type-I and type-V cement (i.e. blended cement) with water-to-cement ratio of 0.4 and 0.43 respectively. The samples were kept in humid chamber at controlled temperature of 20°C before being demolded after 24 hours. Then they were kept in the same chamber for several months. At the end of the curing period, the cylinders were sawed into thin samples. The materials microstructure was characterized through apparent density and water porosity measurements following the protocol [12]. Table 1 gives the results obtained as an average of three measurements.

Table 1: Microstructure characteristics.

Material	Apparent density, kg/m^3	Water porosity
type-I paste	1580	0.39
type-V paste	1594	0.37
TiO_2	3571	0.4

Hugo Mercado-Mendoza: Laboratoire ICube (INSA / Université de Strasbourg), Département Mécanique, Equipe Génie Civil et Energétique, 2 rue Boussingault, F-67000 Strasbourg, France
***Corresponding Author: Sylvie Lorente:** Université de Toulouse, UPS, INSA, LMDC (Laboratoire Matériaux et Durabilité des Constructions), 135 Avenue de Rangueil, F-31077 Toulouse Cedex 04, France, E-mail: lorente@insa-toulouse.fr

This paper was presented during 10th International Conference on Diffusion in Solids and Liquids, June 23-27, 2014, Paris, France.

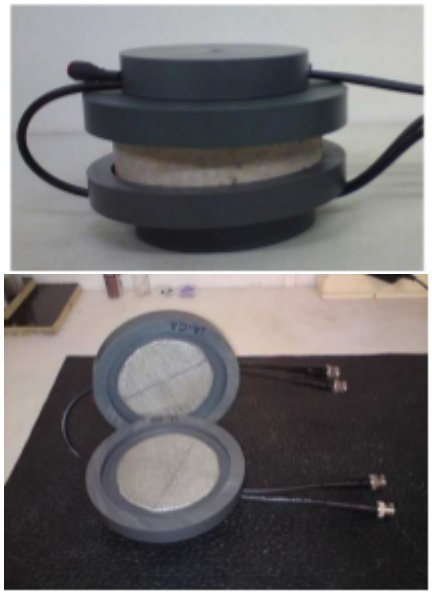

Figure 1: EIS cell.

Cement pastes samples were placed in chambers at controlled relative humidity until equilibrium before being tested with Electrochemical Impedance Spectroscopy. Impedance measurements were performed with an impedance analyzer (HP 4294A), with an amplitude of the sinusoidal voltage of 200 mV, and a frequency range of $40 - 110\,10^6$ Hz. The values of the measured impedance were plotted on Nyquist plots, before analysis. Each electrode was made of copper with a thin mattress of stainless steel, and protected by a PVC envelope (see Figure 1). The mattress of stainless steel was thick and flexible enough to ensure a very good contact with the sample when a light compression was applied between the two PVC containers. The test lasted less than five minutes per sample. Every result presented in this paper corresponds to an average of 3 to 4 tests, one test per day, in a room at constant temperature.

The Nernst-Einstein relation reads

$$\mu = \frac{zFD_{bulk}}{RT}, \tag{1}$$

where D_{bulk} is the diffusion coefficient in an infinitely diluted solution, and μ is the ionic mobility, which is linked to the electrical conductivity σ through [13]

$$\mu = Fz\sigma. \tag{2}$$

The formation factor F_f is the ratio of the pore solution conductivity σ_{bulk} to the conductivity of the material saturated with the same pore solution σ_{mat}. This ratio is the same as the ratio of an ion diffusion coefficient in the pore solution D_{bulk} to the diffusion coefficient of the same ion through the material.

$$F_f = \frac{\sigma_{bulk}}{\sigma_{mat}} = \frac{D_{bulk}}{D}. \tag{3}$$

[14, 15] gave a very good overview on the applicability of the notion of formation factor to cementitious materials. Indeed the formation factor corresponds to a global factor characterizing the pore structure of the material. D_{bulk} is available in books of chemistry (e.g. [13]), while the material conductivity is obtained from

$$\sigma_{mat} = \frac{L}{AR_{mat}}, \tag{4}$$

where A is the sample cross-section, and R_{mat} is the saturated material electrical resistance. As shown in the next section the value of R_{mat} depends on the type of equivalent electrical circuit that is associated with the Nyquist diagram. Whatever the electrical model chosen, the impedance of the equivalent circuit is given by:

$$Z(\omega) = Z_{real}(\omega) + iZ_{imag}(\omega). \tag{5}$$

One of the biggest challenges in electrochemical impedance spectroscopy is to propose an electrical model that not only fits at best the experimental results, but also corresponds to an actual description of the material tested. The difficulty lies in the fact that the solution of the problem is not unique, meaning that several electrical circuits may correspond to the same diagram on the Nyquist plot [16, 17]. The circuit is made of the assembly in series of two blocks: one block describes the material, while the second one represents the electrodes and their interface. The latter is built as the assembly in parallel of a resistance R_E and a constant phase element Q_E. The material itself can be viewed as an assembly of simple electrical elements (Figure 2). It is represented by a combination in parallel of three ways to transfer electrical charges:

- The continuous conductive paths represent the fraction of opened and connected pores. They are represented by a resistance in the equivalent electrical model, R_{CCP} which is the material resistance we are interested in: R_{mat}.
- The solid matrix plays the role of non-ideal capacitor, modeled by a constant phase element Q_{mat}.
- The discontinuous pore paths are pore paths separated by solid layers. The association in series of a resistance R_{CP} and a constant phase element Q_{DP} represents this path, where CP means continuous portion and DP discontinuous point. The microstructure model is then associated in series with the block representing the contribution of the electrodes, as shown in Figure 2.

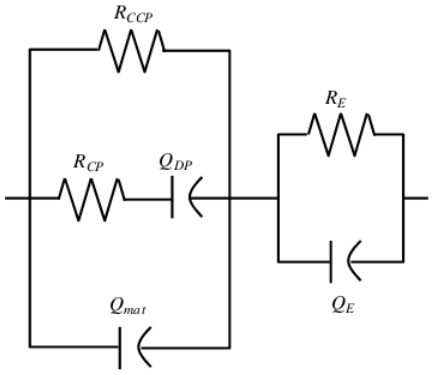

Figure 2: Electrical equivalent microstructural model.

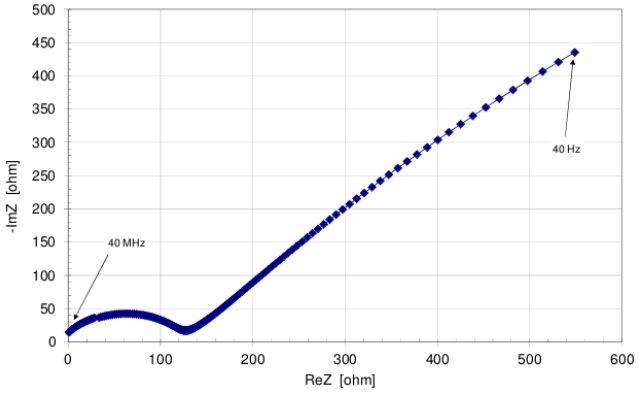

Figure 3: Example of EIS results on TiO_2 sample.

Generally, the impedance of each simple element constituting the equivalent circuit is

$$Z(\omega) = R \tag{6}$$

for the resistance, and

$$Z(\omega) = \frac{1}{Q(i\omega)^{\alpha}} \tag{7}$$

for the constant phase element, where the constant Q is the equivalent capacitance $(1/|Z|)$ at $\omega = 1$ rad/s. As a result, the equivalent impedance of the entire circuit is

$$Z(\omega) = \left(\frac{1}{R_{mat}} + \frac{1}{R_{CP} + \frac{1}{Q_{DP}(i\omega)^{\alpha_{DP}}}} + Q_{mat}(i\omega)^{\alpha_{mat}}\right)^{-1} + \left(\frac{1}{R_E} + Q_E(i\omega)^{\alpha_E}\right)^{-1}. \tag{8}$$

Equation (8) represents both the sample of material and the two electrodes constituting the experiment. This equation contains nine unknowns: the three resistances (R_{mat}, R_{CP}, R_E), the three equivalent capacitances (Q terms), and the three α factors appearing in the constant phase element expressions. The fitting procedure consists of solving the equation

$$Z(\omega) - Z_{exp}(\omega) = 0, \tag{9}$$

where the nine electrical characteristics (R, Q, α) are unknown. The optimization is based on the Simplex algorithm [18, 19]. The code was developed in the Matlab environment. Finally, once R_{mat} is obtained, the diffusion coefficient can be calculated from Equations (3) and (4).

3 Impact of the pore solution composition

Three samples of TiO_2 disks were vacuum saturated (following the protocol [12]) with artificial solutions presented in Table 2.

Figure 3 presents an example of result corresponding to the EIS test of TiO_2 sample. Note that the minimum of the imaginary part is obtained for a frequency of 61593 Hz, leading to an overall material resistance of 126 Ω. The capacitive branch measured in the lower frequencies highlight the effect of the interface between the electrodes and the material. The capacitive loop obtained above ω_{mat} is typical of the material itself [20].

The samples saturated with the first two solutions were dried after the tests and vacuum saturated again with the same solution to which 20 g/L of NaCl was added. This led respectively to ionic strengths of 0.496 mol/L for solution 1 + NaCl, and 0.586 mol/L for solution 2 + NaCl.

The formation factor F_f was determined in each case from the EIS measurements. Its variation is small and in the range of discrepancy of the experiments. The results obtained are gathered in Figure 4. They show that the formation factor of this non-reactive material is not affected by a change in ionic strength, at least in the range of ionic strengths tested. Extending this result to the value of the diffusion coefficient of an ionic species thanks to Equation (3), means that the ionic diffusion coefficient will not vary when the ionic strength of the pore solution changes, thus will not vary when the pore solution concentration of the various ions in presence change. Such results are in agreement with previous works of our group (see for example [21] and [3]).

Table 2: Pore solutions

Solution	Na^+ (mol/m^3)	K^+ (mol/m^3)	OH^- (mol/m^3)	Ionic strength (mol/L)
Solution 1, from type-I cement paste	31.5	122.8	154.3	0.154
Solution 2, from type-V cement paste	70.6	173.9	244.6	0.245
Solution 3	127.6	510.6	638.3	0.638

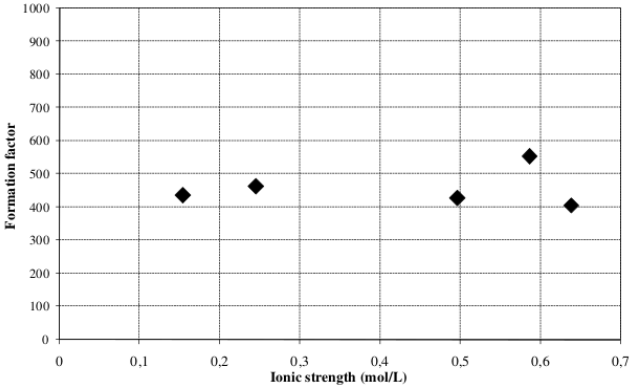

Figure 4: Formation factors as a function of the ionic strength.

4 Impact of the saturation level

We present in Figure 5 the EIS results obtained for the different water saturation levels, S_l in the case of a type I cement paste. Because a test lasts less than 5 minutes, we considered that the saturation state of the material remained constant during the experiment.

When the water saturation level S_l is 97.3%, the results plotted in the Nyquist diagram resemble the ones obtained in the fully saturated state. The two capacitive loops begin to appear clearly in the diagram when S_l = 0.67, while the inflexion of the experimental curve between the second capacitive arc and the part due to electrodes interface becomes smoother.

The diagram for S_l = 0.50 exhibits a drastic change. One capacitive loop is still visible in the highest frequency while the other loop seems to be mixed with what was a tail due to the electrodes for higher water saturation levels. When S_l continues to decrease, the two capacitive arcs are not detectable anymore.

Figure 5 also shows the numerical Nyquist plots corresponding to the Simplex algorithm optimization. The model fits with very good accuracy the experimental results. The microstructure model chosen in this work is robust and describes the material behavior for all the water saturation levels studied.

From the strict viewpoint of determining an ionic diffusion coefficient, the parameter of interest is the one characterizing the continuous conductive paths, R_{mat}. When the porous system is fully saturated or almost fully saturated, the R_{mat} resistance corresponds to the value of the equivalent circuit impedance for which the imaginary part is null, for a frequency located between the two extreme frequency values. This means that there is no need for a sophisticated model to obtain from the Nyquist diagram the information with which the sample diffusion coefficient can be calculated. Note that in practice the equivalent circuit impedance does not have a null imaginary part but rather reaches a minimum value.

As shown in Figure 5, the Nyquist diagram shape changes drastically when the water saturation level decreases. In this case, the electrical model is absolutely necessary because the resistance cannot be extracted directly from the plot, whereas Rmat remains a result from the microstructure-based model for any value of the water saturation level.

The values of the formation factor are presented in Figure 6 as a function of the water saturation level together with the chloride diffusion coefficient. The formation factor is a macroscopic parameter that accounts for the geometry of the porous system through the tortuosity of the network, its constrictivity and connectivity [22, 23]. We see from Figure 6 that it does not remain a constant because its value depends on the electrical conductivity of the pore network; this is why the formation factor gives not only a global image of the pore network geometry but also of the saturation state of the material.

The chloride diffusion coefficient decreases regularly with the saturation level as it can be seen on the log diagram, which means that there is continuity in the liquid fraction all over the sample. From a fully saturated state to S_l = 0.18, the chloride diffusion coefficient decreases by three orders of magnitude, moving from about 1.8×10^{-11} m^2/s to 5.5×10^{-15} m^2/s in the case of the type I cement pastes. The decrease in the diffusion coefficient is sharper in the case of the cement pastes with mineral additions (type V). The diffusion coefficient is of the same order of magnitude when the samples are saturated, but one order of magnitude lower than the type I pastes when the saturation level is of 20%, even though the water porosity of the samples is identical. The difference in results is

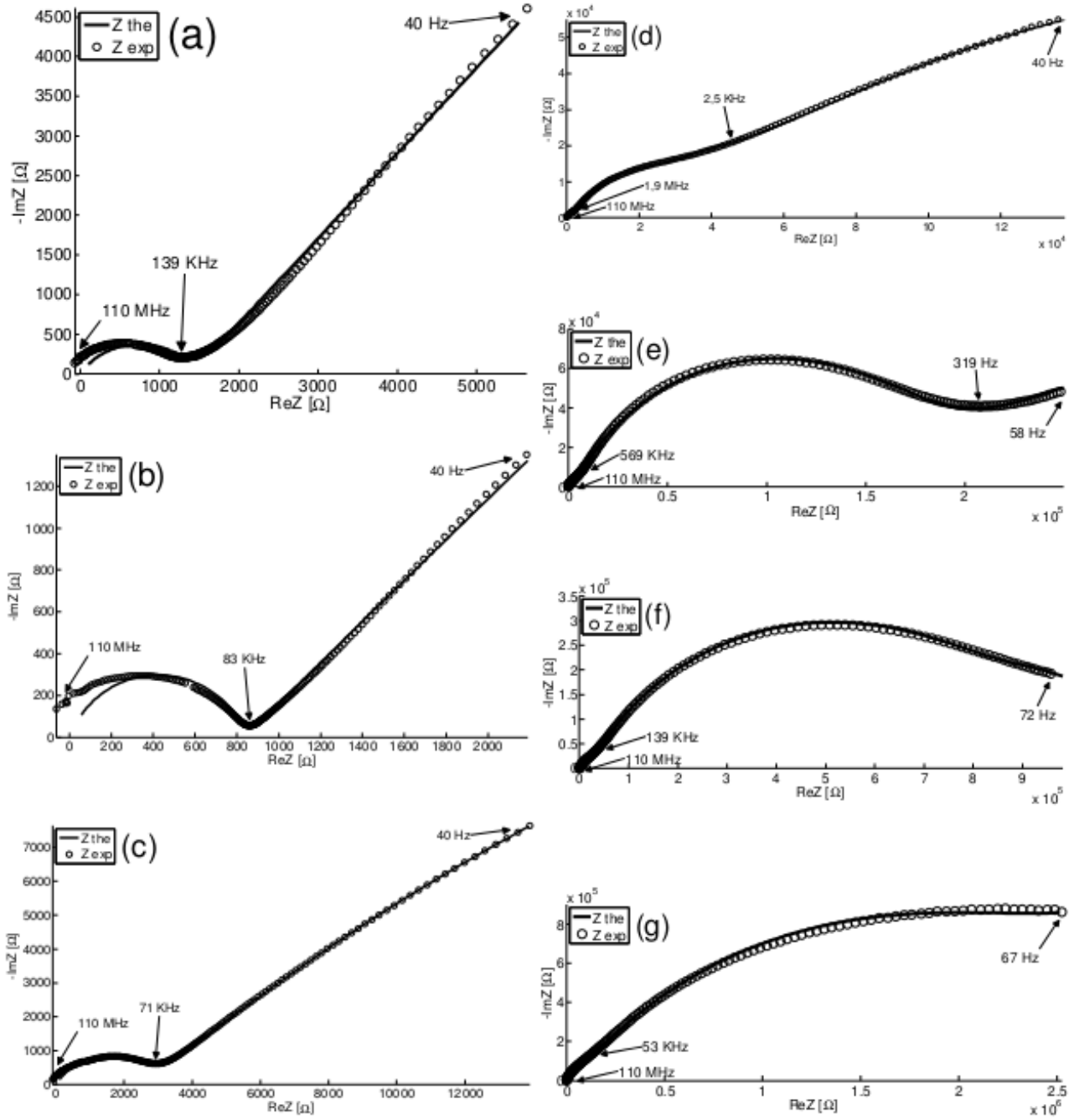

Figure 5: Experimental and modeled Nyquist plots for the different water saturation levels of type I cement paste; (a) S_l = 0.973, (b) S_l = 0.966, (c) S_l = 0.88, (d) S_l = 0.67, (e) S_l = 0.50, (f) S_l = 0.30, (g) S_l = 0.18.

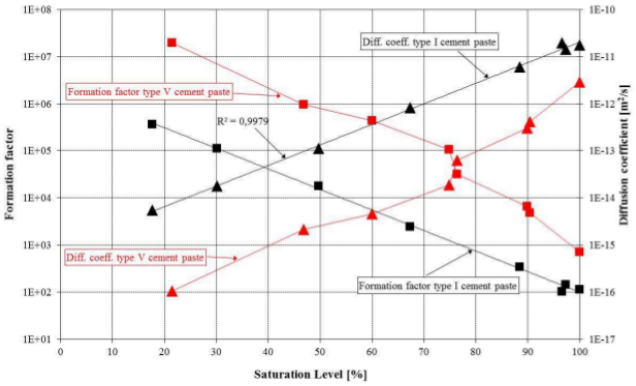

Figure 6: Formation factor and chloride diffusion coefficient as a function of the water saturation level.

to be found in the pore size distribution of such materials. Type V cement pastes possess typically the same total pore volume as type I (see Table 1). Yet, their pore size is much smaller as mercury intrusion porosimetry tests can demonstrate [24] and this make them more sensitive to dryness.

5 Concluding remarks

The objective of this work was to review the progress of our group on the impact of the pore solution on diffusion through saturated and non-saturated materials. The method chosen to characterize diffusion is based on the electrical analogy between current transport and diffusive transport, and uses Electrochemical Impedance Spectroscopy.

The electrical equivalent model based on the material microstructure proved to be robust over the entire range of water saturation levels, capturing the main features of the material microstructure.

Acknowledgement: This work was supported by a contract from ANDRA (Agence Nationale pour la Gestion des Déchets Radioactifs).

Nomenclature

A Sample cross section [m^2]
D_{bulk} Diffusion coefficient in an infinitely diluted solution, [$m^2.s^{-1}$]
F Faraday constant, [$C.mol^{-1}$]
F_f Formation factor, [-]
L Sample thickness, [m]
Q Equivalent capacitance of a constant phase element, [F]
R Ideal gas constant, [$J.mol^{-1}.K^{-1}$]
R Electrical resistance, [Ω]
S_l Saturation level, [-]
T Temperature, [K]
$Z(\omega)$ Impedance [Ω]
z Valency of an ionic species, [-]

Greek letters

α Phase constant of a Q element, [-]
μ Electrochemical mobility of an ionic species, [$m^2.s^{-1}.V^{-1}$]
σ Electrical conductivity, [$S.m^{-1}$]
ω Angular frequency, [$rad.s^{-1}$]

References

[1] Marchand J., Modelling the behaviour of unsaturated cement based systems exposed to aggressive chemical environments, Mater. Struct., 2001, 34, 195–200.
[2] Bégué P., Lorente S., Migration versus diffusion through porous media: time-dependent scale analysis, J. Porous Media, 2006, 9, 637–650.
[3] Voinitchi D., Julien S., Lorente S., The relation between electrokinetics and chloride transport through cement-based materials, Cem. Concr. Compos., 2008, 30, 157–166.
[4] Tang L.P., Nilsson L.O., Rapid determination of the chloride diffusivity in concrete by applying an electrical field, ACI Mater. J., 1992, 89, 49–53.
[5] Khitab A., Lorente S., Ollivier J.P., Predictive model for chloride penetration through concrete, Mag. Concr. Res., 2005, 57(9), 511–520.
[6] Shi M., Chen Z., Sun J., Determination of chloride diffusivity in concrete by AC impedance spectroscopy, Cem. Concr. Res., 1999, 29, 1111–1115.
[7] Sanchez I., Lopez M.P., Ortega J.M., Climent M.A., Impedance spectroscopy: an efficient tool to determine the non-steady-state chloride diffusion coefficient in building materials, Mater. Corros., 2011, 62, 139–145.
[8] Cabeza M., Keddam M., Novoa X.R., Sanchez I., Takenouti H., Impedance spectroscopy to characterize the pore structure during the hardening process of Portland cement paste, Electrochim. Acta, 2006, 51, 1831–1841.
[9] Diaz B., Nóvoa X.R., Pérez M.C., Study of the chloride diffusion in mortar: a new method of determining diffusion coefficients based on impedance measurements, Cem. Concr. Compos., 2006, 28, 237–245.
[10] Vedalakshmi R., Renugha Devi R., Bosco E., Palaniswamy N., Determination of diffusion coefficient of chloride in concrete: an electrochemical impedance spectroscopic approach, Mater.

Struct., 2008, 41, 1315–1326.
[11] Loche J.M., Ammar A., Dumargue P., Influence of the migration of chloride ions on the electrochemical impedance spectroscopy of mortar paste, Cem. Concr. Res., 2005, 35, 1797–1803.
[12] Arliguie G., Hornain H., GranDuBé: Grandeurs associées à la Durabilité des Bétons, Presses de l'école nationale des Ponts et Chaussées, Paris, 2007.
[13] Atkins P. W., Physical chemistry, 6th edition, Oxford university press, Oxford, Melbourne, Tokyo, 1998.
[14] Snyder K.A., Ferraris C., Martyrs N.S., Garboczi E.J., Using impedance spectroscopy to assess the viability of the rapid chloride test for determining concrete conductivity, J. Res. NIST, 2000, 105, 497–509.
[15] Snyder K.A., The relationship between the formation factor and the diffusion coefficient of porous materials saturated with concentrated electrolytes: theoretical and experimental considerations, Concr. Sci. Eng., 2001, 3, 216–224.
[16] Barsoukov E., Macdonald J.R., Impedance spectroscopy, 2nd edition, John Wiley & Sons, Inc., Hoboken, 2005.
[17] Orazem M.E., Tribollet B., Electrochemical impedance spectroscopy, John Wiley & Sons, Inc., Hoboken, 2008.
[18] Nelder J., Mead R., A simplex method for function minimization, Comput. J., 1965, 7, 308–313.
[19] Olsson D., Nelson L., The Nelder-Mead simplex procedure for function minimization, Technometrics, 1975, 17, 45–51.
[20] Cabeza M., Merino P., Miranda A., Nóvoa X.R., Sánchez I., Impedance spectroscopy study of hardened Portland cement paste, Cem. Concr. Res., 2002, 32, 881–91.
[21] Lorente S., Constructal view of electrokinetic transfer through porous media, J. Phys. D.: Appl. Phys., 2007, 40(9), 2941–2947.
[22] Nield D.A., Bejan A., Convection in Porous Media, 3rd edition, Springer, New York, 2006.
[23] Bejan A., Dincer I., Lorente S., Miguel A.F., Reis A.H., Porous and Complex Flow Structures in Modern Technologies, Springer, New York, 2004.
[24] Mercado H., Lorente S., Bourbon X., Chloride diffusion coefficients: a comparison between impedance spectroscopy and electrokinetic tests, Cem. Concr. Compos., 2012, 34, 68–75.